

$T=0$ and $T=1$ pairing in rotational states of the $N=Z$ nucleus ^{80}Zr

Alan L. Goodman

Physics Department, Tulane University, New Orleans, Louisiana 70118

(Received 18 October 2000; published 23 March 2001)

Hartree-Fock-Bogoliubov calculations for the $N=Z$ nucleus ^{80}Zr give a ground state band with $T=1$ Cooper pairs and an excited band with $T=0$ Cooper pairs. The bands cross at spin $I \approx 5\hbar$, providing a ‘‘phase transition’’ from $T=1$ pairs for $I < 5\hbar$ to $T=0$ pairs for $I > 5\hbar$. There is also a $T=0+T=1$ pair band, which forms an envelope to the $T=1$ pair band and the $T=0$ pair band. In this band there is a more gradual transition from $T=1$ pairs at $I=0$ to $T=0$ pairs at high spins, with $T=0$ pairs and $T=1$ pairs coexisting at intermediate spins. The Coriolis antipairing (CAP) effect breaks the $T=1$ pairs, but there is no CAP effect for $T=0$ pairs in which the n and p occupy identical space-spin orbitals. The $T=1$ pair band has a moment of inertia $\mathcal{I}(\omega)$ which backbends at spins between $8\hbar$ and $14\hbar$, but the $T=0$ pair band does not backbend. Both bands have $g_{9/2}$ spin alignments. For the $T=0$ pair band, the dominant angular momentum of a pair is $J=5$, not $J=1$ or $J=J_{max}=9$ as was anticipated. For a rotating $N=Z$ =even nucleus, $T=0$ pairing produces a twofold degeneracy in the canonical orbital occupation probability v^2 , although $T=1$ pairing produces a fourfold degeneracy in v^2 .

DOI: 10.1103/PhysRevC.63.044325

PACS number(s): 21.60.-n

I. INTRODUCTION

Most nonrotating atomic nuclei are superfluids, in which each Cooper pair contains two neutrons or two protons, and each pair has isospin $T=1$. However, the introduction of radioactive nuclear beams and more sensitive detectors has generated an intense search for superfluid nuclei in which each Cooper pair contains one neutron and one proton, where each neutron-proton pair may have $T=1$ or $T=0$ [1]. The most likely candidates for neutron-proton pairing are $N=Z$ nuclei, where the neutrons and protons occupy identical space-spin orbitals, and have maximum spatial overlap. One possible signature for neutron-proton pairing may be the response of the nucleus to a rotation [2–15]. Rotation might affect $T=0$ pairs in a different manner than $T=1$ pairs. This could provide an observable distinction between $T=0$ pairs and $T=1$ pairs.

This article calculates the rotational states of the $N=Z$ nucleus ^{80}Zr . The isospin T and angular momentum J of the Cooper pairs will be determined for each nuclear yrast state with spin I . (Throughout this article T refers to the isospin of one pair of nucleons, not the isospin of the nucleus.) The conventional yrast line, which permits only neutron-neutron and proton-proton pairs, will be compared to the yrast line which also permits neutron-proton pairs.

The following questions will be addressed: Are there significant alterations in the yrast line when neutron-proton pairs are permitted? Does the competition between $T=1$ pairing and $T=0$ pairing cause substantial changes in the yrast line? Does the inclusion of neutron-proton pairs cause the yrast line of ^{80}Zr to have a ‘‘phase transition’’? If $T=0$ Cooper pairs exist, is their angular momentum either $J=1$ or $J=J_{max}=2j$ (where j is the nucleon spin), as is often stated, or do they have another value for J ? For a rotating $N=Z$ =even nucleus, do $T=0$ pairs generate a density matrix ρ which has the same degeneracy as would occur for $T=1$ pairs; i.e., does the canonical orbital occupation prob-

ability v^2 have the same degeneracy for $T=0$ pairs as for $T=1$ pairs? How significant is the time-reversal symmetry breaking in the rotating $T=0$ pair potential? In a rotating nucleus with $T=1$ pairing, the lowest quasiparticle energy usually vanishes at a critical rotational frequency; does this also occur for $T=0$ pairing? If a rotational band has a moment of inertia which does not backbend or upbend, does it necessarily follow that this band has no spin alignments?

II. HARTREE-FOCK-BOGOLIUBOV THEORY**A. Cooper pairs**

The nonrotating Hartree-Fock-Bogoliubov (HFB) states of ^{80}Zr with spin $I=0$ were calculated in Refs. [16,17]. The state with the lowest energy, i.e., the ground state, has a prolate deformation and contains only $T=1$ Cooper pairs. For convenience these pairs are chosen as neutron-neutron and proton-proton pairs. (Including $T=1$ neutron-proton pairs makes absolutely no difference in the energy, since the nucleon-nucleon interaction is isospin invariant and $N=Z$.) The nonrotating even-even wave function is time reversal invariant. So the Cooper pairs are $|\alpha n, \bar{\alpha} n, T=1\rangle$ and $|\alpha p, \bar{\alpha} p, T=1\rangle$, where $|\alpha\rangle$ is a HFB canonical space-spin orbital and $|\bar{\alpha}\rangle$ is the time reverse of $|\alpha\rangle$. These are $n\bar{n}$ pairs and $p\bar{p}$ pairs, where the bar indicates that the second nucleon in a pair occupies a space-spin orbital which is the time reverse of the first nucleon’s orbital. Rotation breaks the time-reversal symmetry. Then the Cooper pairs are $|\alpha n, \hat{\alpha} n, T=1\rangle$ and $|\alpha p, \hat{\alpha} p, T=1\rangle$, where $|\hat{\alpha}\rangle$ is not the time reverse of $|\alpha\rangle$. These are $n\hat{n}$ pairs and $p\hat{p}$ pairs, where the hat indicates that the orbital of the second nucleon in a pair is not the time reverse of the first nucleon’s orbital. The orbitals $|\alpha\rangle$ and $|\hat{\alpha}\rangle$ depend upon the rotational frequency ω .

At spin $I=0$ there is an HFB excited state with excitation energy $E=0.645$ MeV. This state has a prolate deformation and contains only $T=0$ neutron-proton pairs. This state is

time-reversal invariant, and contains the Cooper pairs $|\alpha n, \alpha p, T=0\rangle$ and $|\bar{\alpha} n, \bar{\alpha} p, T=0\rangle$. The two nucleons in each pair occupy *identical* space-spin orbitals. The orbitals in the second pair are the time reverse of the orbitals in the first pair. These are np pairs and $\bar{n}\bar{p}$ pairs. Rotation breaks the time-reversal symmetry. Then the pairs are $|\alpha n, \alpha p, T=0\rangle$ and $|\hat{\alpha} n, \hat{\alpha} p, T=0\rangle$, where the orbitals in the second pair are no longer the time reverse of the orbitals in the first pair. However, the two nucleons in each pair still occupy *identical* space-spin orbitals, which depend upon the rotational frequency ω . These are np pairs and $\hat{n}\hat{p}$ pairs.

At spin $I=0$ there is another HFB excited state with excitation energy $E=1.579$ MeV. This state has a prolate deformation and contains only $T=0$ neutron-proton pairs, which are $|\alpha n, \bar{\alpha} p, T=0\rangle$ and $|\alpha p, \bar{\alpha} n, T=0\rangle$. The two nucleons in each pair occupy orbitals which are related by time reversal. The two nucleons in each pair do not occupy identical orbitals. These are $n\bar{p}$ pairs and $p\bar{n}$ pairs. Rotation breaks the time-reversal symmetry. Then the pairs become $|\alpha n, \hat{\alpha} p, T=0\rangle$ and $|\alpha p, \hat{\alpha} n, T=0\rangle$. These are $n\hat{p}$ pairs and $p\hat{n}$ pairs. These pair states exist only up to nuclear spin $I=1$ and vanish at $I=2$.

B. Quasiparticle transformation

These calculations for ^{80}Zr show $n\hat{n}$ pairs, $p\hat{p}$ pairs, and $np(T=0)$ pairs for nuclear spin $I\geq 2$. However, they do not show $n\hat{p}(T=0)$ and $T=1$ pairs for $I\geq 2$. Of course $np(T=1)$ pairs (where n and p occupy identical space-spin orbitals) are forbidden by the Pauli exclusion principle. Consequently the formalism presented here will be restricted to $n\hat{n}$ pairs, $p\hat{p}$ pairs, and $np(T=0)$ pairs in rotating nuclei. The calculations were performed in the basis $|k\rangle = |nljm\rangle$. However, the formalism acquires a simpler form when it is given in the basis of eigenvectors of the reflection symmetry operator σ_x , which are

$$|K\rangle = 2^{-1/2} [|k\rangle + |\bar{k}\rangle], \quad (2.1)$$

$$|\bar{K}\rangle = 2^{-1/2} [-|k\rangle + |\bar{k}\rangle], \quad (2.2)$$

where $|k\rangle$ is now restricted to states where $m-1/2$ equals an even integer, $|\bar{k}\rangle$ is the time reverse of $|k\rangle$, and $|\bar{K}\rangle$ is the time reverse of $|K\rangle$. It was demonstrated in Refs. [18,19] that this $|K\rangle, |\bar{K}\rangle$ basis greatly simplifies the HFB formalism for $n\hat{n}$ pairs and $p\hat{p}$ pairs in rotating nuclei.

Parity is a conserved symmetry. For each parity, the quasiparticle operators a^\dagger are defined by a unitary transformation of the particle operators C^\dagger ,

$$\begin{pmatrix} a^\dagger \\ \mathbf{a} \end{pmatrix} = \begin{pmatrix} U & V \\ V^* & U^* \end{pmatrix} \begin{pmatrix} C^\dagger \\ \mathbf{C} \end{pmatrix}, \quad (2.3)$$

where the vectors \mathbf{a}^\dagger and \mathbf{C}^\dagger are

$$\mathbf{a}^\dagger = \begin{pmatrix} a_1^\dagger \\ a_2^\dagger \\ a_1^\dagger \\ a_2^\dagger \end{pmatrix}, \quad \mathbf{C}^\dagger = \begin{pmatrix} C_p^\dagger \\ C_n^\dagger \\ C_p^\dagger \\ C_n^\dagger \end{pmatrix}. \quad (2.4)$$

The vector \mathbf{C}_p^\dagger has dimension M and contains the components C_{Kp}^\dagger , where M is the number of single proton states $|K\rangle$, and similarly for the vector \mathbf{C}_n^\dagger . The vector \mathbf{C}_p^\dagger has dimension M and contains the components $C_{\bar{K}p}^\dagger$, and similarly for the vector \mathbf{C}_n^\dagger . The vector \mathbf{a}_1^\dagger has dimension M with components a_{j1}^\dagger , where $j=1,2,\dots,M$, and similarly for \mathbf{a}_2^\dagger , \mathbf{a}_1^\dagger , and \mathbf{a}_2^\dagger . For a nucleus with $N=Z$ even, isospin symmetry creates a degeneracy factor of 2 in the quasiparticle energies. Then the matrices U and V have the forms

$$U = \begin{pmatrix} U_1 & 0 & 0 & 0 \\ 0 & U_1 & 0 & 0 \\ 0 & 0 & \hat{U}_1 & 0 \\ 0 & 0 & 0 & \hat{U}_1 \end{pmatrix}, \quad (2.5)$$

$$V = - \begin{pmatrix} 0 & V_1 & V_2 & 0 \\ -V_1 & 0 & 0 & -V_2 \\ -\hat{V}_2 & 0 & 0 & \hat{V}_1 \\ 0 & \hat{V}_2 & -\hat{V}_1 & 0 \end{pmatrix}, \quad (2.6)$$

where the matrices U_1 , V_1 , and V_2 have dimension $M \times M$. It should be emphasized that the matrices U and V are functions of the rotational frequency ω . The quasiparticle operators a^\dagger are spin dependent. The matrices U_1 and V_2 are real. Permitting the matrix V_1 to be complex creates no change in the energy of this state in ^{80}Zr , so V_1 is chosen to be real. (The amplitude V_1 describes the $np(T=0)$ pairs. The isospin generalized BCS theory [20] has a complex amplitude v_1 for these pairs. For other nuclei, a complex v_1 sometimes permits a lower energy, but for most nuclei the energy is not lowered with a complex v_1 .) Combining Eqs. (2.3)–(2.6), the quasiparticle operators are explicitly given as

$$a_{j1}^\dagger = \sum_K [(U_1)_{jK} C_{\bar{K}p}^\dagger - (V_1)_{jK} C_{Kn} - (V_2)_{jK} C_{\bar{K}p}], \quad (2.7)$$

$$a_{j2}^\dagger = \sum_K [(U_1)_{jK} C_{Kn}^\dagger + (V_1)_{jK} C_{Kp} + (V_2)_{jK} C_{\bar{K}n}], \quad (2.8)$$

$$a_{j1}^\dagger = \sum_K [(\hat{U}_1)_{jK} C_{\bar{K}p}^\dagger + (\hat{V}_2)_{jK} C_{Kp} - (\hat{V}_1)_{jK} C_{\bar{K}n}], \quad (2.9)$$

$$a_{j2}^\dagger = \sum_K [(\hat{U}_1)_{jK} C_{\bar{K}n}^\dagger - (\hat{V}_2)_{jK} C_{Kn} + (\hat{V}_1)_{jK} C_{\bar{K}p}]. \quad (2.10)$$

If the rotational frequency $\omega=0$, then $\hat{U}_1=U_1$, $\hat{V}_1=V_1$, and $\hat{V}_2=V_2$. This is the time-reversal symmetry. However, for a rotating nucleus with $\omega \neq 0$, the time-reversal symmetry is broken, so that $\hat{U}_1 \neq U_1$, $\hat{V}_1 \neq V_1$, and $\hat{V}_2 \neq V_2$.

The density matrix and the pairing tensor,

$$\rho_{ij} = \langle C_j^\dagger C_i \rangle, \quad (2.11)$$

$$t_{ij} = \langle C_j C_i \rangle, \quad (2.12)$$

are evaluated with respect to the spin-dependent HFB quasi-particle vacuum, so that

$$\rho = V^\dagger V, \quad (2.13)$$

$$t = V^\dagger U. \quad (2.14)$$

They are functions of the rotational frequency ω . Substituting Eq. (2.6) into Eq. (2.13), and using the unitarity constraint

$$U^\dagger U + \tilde{V} V^* = I, \quad (2.15)$$

it follows that ρ is block diagonal

$$\rho = \begin{pmatrix} \rho_{pp} & 0 & 0 & 0 \\ 0 & \rho_{pp} & 0 & 0 \\ 0 & 0 & \rho_{\bar{p}\bar{p}} & 0 \\ 0 & 0 & 0 & \rho_{\bar{p}\bar{p}} \end{pmatrix}, \quad (2.16)$$

where

$$(\rho_{\tau_1 \tau_2})_{K_1 K_2} = \rho_{K_1 \tau_1, K_2 \tau_2}, \quad (\rho_{\bar{\tau}_1 \bar{\tau}_2})_{K_1 K_2} = \rho_{\bar{K}_1 \tau_1, \bar{K}_2 \tau_2}, \quad (2.17)$$

τ is n or p , and

$$\rho_{pp} = \rho_{nn} = V_1^\dagger V_1 + \hat{V}_2^\dagger \hat{V}_2, \quad (2.18)$$

$$\rho_{\bar{p}\bar{p}} = \rho_{\bar{n}\bar{n}} = \hat{V}_1^\dagger \hat{V}_1 + V_2^\dagger V_2. \quad (2.19)$$

The $M \times M$ matrices ρ_{pp} and $\rho_{\bar{p}\bar{p}}$ are real and symmetric. If $\omega=0$, then $\hat{V}_1=V_1$ and $\hat{V}_2=V_2$, so that $\rho_{pp}=\rho_{\bar{p}\bar{p}}$. This is the time-reversal symmetry. However, for a rotating nucleus where $\omega \neq 0$, then $\hat{V}_1 \neq V_1$ and $\hat{V}_2 \neq V_2$, so that $\rho_{pp} \neq \rho_{\bar{p}\bar{p}}$. The time-reversal symmetry is broken.

The pairing tensor is obtained by substituting Eqs. (2.5) and (2.6) into Eq. (2.14), so that

$$t = \begin{pmatrix} 0 & t_{pn} & t_{p\bar{p}} & 0 \\ -t_{pn} & 0 & 0 & -t_{p\bar{p}} \\ -\tilde{t}_{p\bar{p}} & 0 & 0 & t_{pn} \\ 0 & \tilde{t}_{p\bar{p}} & -t_{pn} & 0 \end{pmatrix}, \quad (2.20)$$

where

$$(t_{\tau_1 \tau_2})_{K_1 K_2} = t_{K_1 \tau_1, K_2 \tau_2}, \quad (t_{\bar{\tau}_1 \bar{\tau}_2})_{K_1 K_2} = t_{K_1 \tau_1, \bar{K}_2 \tau_2}, \quad (2.21)$$

$$(t_{\bar{\tau}_1 \bar{\tau}_2})_{K_1 K_2} = t_{\bar{K}_1 \tau_1, \bar{K}_2 \tau_2},$$

and

$$t_{p\bar{p}} = -t_{n\bar{n}}, \quad (2.22)$$

$$t_{pn} = V_1^\dagger U_1, \quad (2.23)$$

$$t_{p\bar{p}} = \hat{V}_1^\dagger \hat{U}_1, \quad (2.24)$$

$$t_{p\bar{p}} = \hat{V}_2^\dagger \hat{U}_1. \quad (2.25)$$

The matrices t_{pn} , $t_{p\bar{p}}$, and $t_{n\bar{n}}$ have dimension $M \times M$ and are real. The matrices t_{pn} and $t_{p\bar{p}}$ are symmetric. If $\omega=0$, then time-reversal symmetry gives $t_{pn}=t_{p\bar{p}}$. However, if $\omega \neq 0$, then time-reversal symmetry is broken, and $t_{pn} \neq t_{p\bar{p}}$. If $\omega=0$, then time-reversal symmetry causes $t_{p\bar{p}}$ to be symmetric. However, if $\omega \neq 0$, then $t_{p\bar{p}}$ is not symmetric.

The Hartree-Fock (HF) Hamiltonian and HF potential are

$$h = e + \mathcal{U}, \quad (2.26)$$

$$\mathcal{U}_{ij} = \sum_{kl} \langle ik | v_a | jl \rangle \rho_{lk}. \quad (2.27)$$

The isospin structure of h is the same as that of the density matrix ρ in Eq. (2.16). The pair potential is

$$\Delta_{ij} = \frac{1}{2} \sum_{kl} \langle ij | v_a | kl \rangle t_{kl}. \quad (2.28)$$

The isospin structure of Δ is the same as that of the pairing tensor t in Eq. (2.20). Both h and Δ depend upon the rotational frequency ω . For each value of ω , the HFB energy is

$$E_{\text{HFB}} = \langle H \rangle = \text{Tr} \left[\left(e + \frac{1}{2} \mathcal{U} \right) \rho + \frac{1}{2} \Delta t^\dagger \right]. \quad (2.29)$$

The HFB equation is

$$\begin{pmatrix} (h - \lambda - \omega J_x) & \Delta \\ -\Delta^* & -(h - \lambda - \omega J_x)^* \end{pmatrix} \begin{pmatrix} U_j \\ V_j \end{pmatrix} = E_j \begin{pmatrix} U_j \\ V_j \end{pmatrix}. \quad (2.30)$$

The chemical potentials λ_p and λ_n are adjusted so that the number operators N_p and N_n have the correct expectation values. The HFB mean field approximation is used, and particle number projection is not included.

C. Limiting case: $np(T=0)$ pairs

For a $N=Z=$ even nucleus, consider the case where there are only $np(T=0)$ pairs, where the neutron and proton in each pair occupy identical space-spin orbitals if the rotational frequency $\omega=0$. There are no $n\bar{n}$ pairs or $p\bar{p}$ pairs. This is achieved by choosing $V_1 \neq 0$ and $V_2 = 0$ in the initial trial wave function. Then the final self-consistent wave func-

tion will have the same properties. Then the density matrix of Eqs. (2.18) and (2.19) reduces to

$$\rho_{pp} = \rho_{nn} = V_1^\dagger V_1, \quad (2.31)$$

$$\rho_{p\bar{p}} = \rho_{n\bar{n}} = \hat{V}_1^\dagger \hat{V}_1. \quad (2.32)$$

The only nonzero components of the pairing tensor are t_{pn} and $t_{p\bar{n}}$, given by Eqs. (2.23) and (2.24).

1. Canonical representation

The Bloch-Messiah theorem [21] states that any HFB quasiparticle vacuum may be expressed in BCS form, where each paired orbital is paired with only one other orbital. That is, there exists a single-particle basis such that ρ is diagonal and t has nonzero components only between paired orbitals. This is the canonical representation.

For a nonrotating $N=Z$ =even nucleus, time-reversal symmetry and isospin symmetry generate a fourfold degeneracy in the single-particle orbital energies. Then the pairs are $np(T=0)$ and $\bar{n}\bar{p}(T=0)$, where the orbitals in the second pair are the time-reverse of the orbitals in the first pair. Also the four orbitals $|\alpha n\rangle$, $|\alpha p\rangle$, $|\bar{\alpha} n\rangle$, and $|\bar{\alpha} p\rangle$ have identical occupation probabilities v_α^2 . Since J_x is not time-reversal invariant, in a rotating nucleus the $np(T=0)$ pairs cannot be related by time reversal. It is therefore interesting to determine the nature of the correlated $np(T=0)$ pairs in a rotating nucleus.

The HFB unitarity constraint is

$$R^2 = R, \quad (2.33)$$

where R is the generalized density matrix

$$R = \begin{pmatrix} \rho & t \\ t^\dagger & 1 - \tilde{\rho} \end{pmatrix}. \quad (2.34)$$

From Eq. (2.33) it follows that

$$\rho - \rho^2 = t t^\dagger \equiv \theta, \quad (2.35)$$

$$\rho t = t \tilde{\rho}. \quad (2.36)$$

Substitute Eqs. (2.16) and (2.20) into Eq. (2.35), using $t_{p\bar{p}} = 0$, $\rho_{pp} = \rho_{nn}$, and $\rho_{p\bar{p}} = \rho_{n\bar{n}}$. The result is

$$\rho_{pp} - \rho_{pp}^2 = \rho_{nn} - \rho_{nn}^2 = t_{pn} t_{pn}^\dagger \equiv \theta_{pn}, \quad (2.37)$$

$$\rho_{p\bar{p}} - \rho_{p\bar{p}}^2 = \rho_{n\bar{n}} - \rho_{n\bar{n}}^2 = t_{p\bar{n}} t_{p\bar{n}}^\dagger \equiv \theta_{p\bar{n}}. \quad (2.38)$$

Note that θ_{pn} and $\theta_{p\bar{n}}$ are hermitian. From Eq. (2.37) it follows that θ_{pn} commutes with ρ_{pp} and ρ_{nn} . Consequently they can be diagonalized by the same unitary transformation. The eigenvectors of ρ_{pp} are

$$|\alpha p\rangle = \sum_K D_{\alpha K} |Kp\rangle, \quad (2.39)$$

and the eigenvectors of ρ_{nn} are

$$|\alpha n\rangle = \sum_K D_{\alpha K} |Kn\rangle. \quad (2.40)$$

The corresponding eigenvalues of ρ_{pp} and ρ_{nn} are

$$\rho_\alpha = v_\alpha^2. \quad (2.41)$$

From Eq. (2.37) it follows that the eigenvalues of θ_{pn} are

$$\theta_\alpha = \rho_\alpha - \rho_\alpha^2 = v_\alpha^2(1 - v_\alpha^2). \quad (2.42)$$

Equations (2.39)–(2.41) show that even in a rotating nucleus, a neutron and a proton occupy *identical* space-spin orbitals $|\alpha\rangle$ with equal occupation probability v_α^2 , where $|\alpha\rangle$ and v_α^2 depend upon ω . In a similar manner, it follows from Eq. (2.38) that the eigenvectors of $\rho_{p\bar{p}}$ are

$$|\hat{\alpha} p\rangle = \sum_K \hat{D}_{\alpha K} |\bar{K}p\rangle, \quad (2.43)$$

and the eigenvectors of $\rho_{n\bar{n}}$ are

$$|\hat{\alpha} n\rangle = \sum_K \hat{D}_{\alpha K} |\bar{K}n\rangle. \quad (2.44)$$

The corresponding eigenvalues of $\rho_{p\bar{p}}$ and $\rho_{n\bar{n}}$ are

$$\rho_{\hat{\alpha}} = v_{\hat{\alpha}}^2. \quad (2.45)$$

From Eq. (2.38) it follows that the eigenvalues of $\theta_{p\bar{n}}$ are

$$\theta_{\hat{\alpha}} = \rho_{\hat{\alpha}} - \rho_{\hat{\alpha}}^2 = v_{\hat{\alpha}}^2(1 - v_{\hat{\alpha}}^2). \quad (2.46)$$

Equations (2.43)–(2.45) show that even in a rotating nucleus, a neutron and a proton occupy *identical* space-spin orbitals $|\hat{\alpha}\rangle$ with equal occupation probability $v_{\hat{\alpha}}^2$, where $|\hat{\alpha}\rangle$ and $v_{\hat{\alpha}}^2$ depend upon ω . For a nonrotating nucleus with $\omega=0$, time-reversal symmetry gives $\hat{D}=D$, so that $|\hat{\alpha}\rangle=|\bar{\alpha}\rangle$, as well as $v_{\hat{\alpha}}^2=v_\alpha^2$. The density matrix ρ is fourfold degenerate. However, for a rotating nucleus with $\omega \neq 0$, the time-reversal symmetry is broken, so that $\hat{D} \neq D$, $|\hat{\alpha}\rangle \neq |\bar{\alpha}\rangle$, and $v_{\hat{\alpha}}^2 \neq v_\alpha^2$. The density matrix ρ is only twofold degenerate.

In 1974 [18] it was proven that for $n\hat{n}$ pairs and $p\hat{p}$ pairs in a rotating nucleus, the density matrix ρ is fourfold degenerate, with $v_{\hat{\alpha}}^2 = v_\alpha^2$, even though the time-reversal symmetry is broken in the density matrix ρ , with $\rho_{pp} \neq \rho_{p\bar{p}}$. So the result shown here that ρ is only twofold degenerate for a rotating nucleus with $np(T=0)$ pairs (where the neutron and proton in a pair occupy identical orbitals) is interesting. It demonstrates that the pairing tensor t has a fundamentally different structure for $p\hat{p}$ pairs and $np(T=0)$ pairs (where the two nucleons occupy identical orbitals), and that this difference acts through the unitarity constraint [Eq. (2.33)] to alter the degeneracy of the density matrix ρ .

Substitute Eqs. (2.16) and (2.20) into Eq. (2.36), using $t_{p\bar{p}} = 0$, $\rho_{pp} = \rho_{nn}$, and $\rho_{p\bar{p}} = \rho_{n\bar{n}}$. The result is

$$\rho_{pp} t_{pn} = t_{pn} \tilde{\rho}_{nn}, \quad (2.47)$$

$$\rho_{pp}^- t_{pn}^- = t_{pn}^- \tilde{\rho}_{nn}^- . \quad (2.48)$$

Express Eq. (2.47) in the $|\alpha\rangle$ basis and Eq. (2.48) in the $|\hat{\alpha}\rangle$ basis, so that

$$(t_{pn})_{\alpha\alpha'} [(\rho_{pp})_{\alpha\alpha} - (\rho_{nn})_{\alpha'\alpha'}] = (t_{pn})_{\alpha\alpha'} [\rho_{\alpha} - \rho_{\alpha'}] = 0, \quad (2.49)$$

$$(t_{pn}^-)_{\hat{\alpha}\hat{\alpha}'} [(\rho_{pp}^-)_{\hat{\alpha}\hat{\alpha}} - (\rho_{nn}^-)_{\hat{\alpha}'\hat{\alpha}'}] = (t_{pn}^-)_{\hat{\alpha}\hat{\alpha}'} [\rho_{\hat{\alpha}} - \rho_{\hat{\alpha}'}] = 0. \quad (2.50)$$

The pairing tensor t_{pn} has nonzero components only between states $|\alpha p\rangle$ and $|\alpha n\rangle$ having the same occupation probability v_{α}^2 . The pairing tensor t_{pn}^- has nonzero components only between states $|\hat{\alpha} p\rangle$ and $|\hat{\alpha} n\rangle$ having the same occupation probability $v_{\hat{\alpha}}^2$.

From these results on the structure of the density matrix ρ and pairing tensor t , it follows that the HFB quasiparticle vacuum can be expressed as

$$|\Phi_0\rangle = \prod_{\alpha>0} (u_{\alpha} + v_{\alpha} C_{ap}^{\dagger} C_{an}^{\dagger}) (u_{\hat{\alpha}} + v_{\hat{\alpha}} C_{\hat{a}p}^{\dagger} C_{\hat{a}n}^{\dagger}) |0\rangle, \quad (2.51)$$

where $u_{\alpha}^2 + v_{\alpha}^2 = 1$, $u_{\hat{\alpha}}^2 + v_{\hat{\alpha}}^2 = 1$, and the orbitals $|\alpha\rangle$ and $|\hat{\alpha}\rangle$ are given by Eqs. (2.39) and (2.43). The canonical orbitals $|\alpha\rangle$ are not imposed *a priori*, but instead are determined by the final self-consistent HFB density matrix ρ . It should be remembered that this is a spin-dependent state, where the orbitals and their occupation probabilities depend upon the rotational frequency ω . The nonzero elements of the density matrix are $\rho_{\alpha p, \alpha p} = \rho_{\alpha n, \alpha n} = v_{\alpha}^2$ and $\rho_{\hat{\alpha} p, \hat{\alpha} p} = \rho_{\hat{\alpha} n, \hat{\alpha} n} = v_{\hat{\alpha}}^2$. The nonzero elements of the pairing tensor are $t_{\alpha p, \alpha n} = u_{\alpha} v_{\alpha}$ and $t_{\hat{\alpha} p, \hat{\alpha} n} = u_{\hat{\alpha}} v_{\hat{\alpha}}$. For a rotating nucleus where $\omega \neq 0$, the time-reversal symmetry is broken, so that $|\hat{\alpha}\rangle \neq |\bar{\alpha}\rangle$, $u_{\hat{\alpha}} \neq u_{\alpha}$, and $v_{\hat{\alpha}} \neq v_{\alpha}$. For a nonrotating nucleus where $\omega = 0$, the time-reversal symmetry is restored, so that $|\hat{\alpha}\rangle = |\bar{\alpha}\rangle$, $u_{\hat{\alpha}} = u_{\alpha}$, and $v_{\hat{\alpha}} = v_{\alpha}$. Then the wave function simplifies to

$$|\Phi_0\rangle = \prod_{\alpha>0} (u_{\alpha} + v_{\alpha} C_{ap}^{\dagger} C_{an}^{\dagger}) (u_{\alpha} + v_{\alpha} C_{\bar{a}p}^{\dagger} C_{\bar{a}n}^{\dagger}) |0\rangle. \quad (2.52)$$

In wave functions (2.51) and (2.52) both orbitals in a given pair have the same occupation v_{α}^2 (or $v_{\hat{\alpha}}^2$). Therefore these wave functions contain no blocked orbitals. (A blocked orbital occurs when one orbital in a pair is fully occupied, i.e., $v^2 = 1$, and the other orbital in the same pair is empty, i.e., $v^2 = 0$.) These wave functions do not exhibit the blocking effect which is characteristic of odd-odd nuclei.

2. Breaking of time-reversal symmetry

For a nonrotating $N=Z$ =even nucleus with $\omega=0$, time-reversal symmetry is preserved in the densities ρ and t and in the mean fields h and Δ . However, when the nucleus rotates with $\omega \neq 0$, the cranking term $-\omega J_x$ breaks the time-reversal symmetry in the densities and mean fields. It is then interesting to determine the extent of the time-reversal violation by

breaking the densities and fields into time-reversal even and time-reversal odd components.

Define

$$\rho_{pp}^{(\pm)} = \frac{1}{2} (\rho_{pp} \pm \rho_{pp}^-). \quad (2.53)$$

Then from Eqs. (2.17) and (2.53) it follows that

$$T \rho_{pp}^{(\pm)} T^{-1} = \pm \rho_{pp}^{(\pm)}, \quad (2.54)$$

where T is the time-reversal operator, and $(TMT^{-1})_{ij} \equiv M_{\bar{i}\bar{j}}$ for any matrix M . Therefore $\rho_{pp}^{(+)}$ and $\rho_{pp}^{(-)}$ are the time-reversal even and odd components of ρ_{pp} . The matrices $\rho_{pp}^{(+)}$ and $\rho_{pp}^{(-)}$ are real and symmetric. It follows from Eqs. (2.1) and (2.2) that

$$(\rho_{pp}^{(+)})_{KK'} = (\rho_{pp})_{kk'}, \quad (2.55)$$

$$(\rho_{pp}^{(-)})_{KK'} = (\rho_{pp})_{k\bar{k}'}. \quad (2.56)$$

For a nonrotating nucleus with $\omega=0$, then $\rho_{pp}^{(-)}=0$. For a rotating nucleus with $\omega \neq 0$, then $\rho_{pp}^{(-)} \neq 0$. In a rotating nucleus, Eq. (2.16) shows that $\rho_{K\bar{K}'}=0$; however, Eq. (2.56) shows that $\rho_{k\bar{k}'} \neq 0$. This demonstrates that the $|K\rangle$, $|\bar{K}\rangle$ basis reduces the dimension of ρ by a factor of 2, compared to the $|k\rangle$, $|\bar{k}\rangle$ basis, for a rotating nucleus. The Hartree-Fock Hamiltonian h separates into time-reversal even and odd components in the same manner as ρ , so that

$$h_{pp}^{(\pm)} = \frac{1}{2} (h_{pp} \pm h_{pp}^-). \quad (2.57)$$

Also, one can substitute h for ρ in Eqs. (2.54)–(2.56).

Define

$$t_{pn}^{(\pm)} = \frac{1}{2} (t_{pn} \pm t_{pn}^-). \quad (2.58)$$

Then from Eqs. (2.21) and (2.58) it follows that

$$T t_{pn}^{(\pm)} T^{-1} = \pm t_{pn}^{(\pm)}. \quad (2.59)$$

Therefore $t_{pn}^{(+)}$ and $t_{pn}^{(-)}$ are the time-reversal even and odd components of t_{pn} . The matrices $t_{pn}^{(+)}$ and $t_{pn}^{(-)}$ are real and symmetric. It follows from Eqs. (2.1) and (2.2) that

$$(t_{pn}^{(+)})_{KK'} = (t_{pn})_{kk'}, \quad (2.60)$$

$$(t_{pn}^{(-)})_{KK'} = (t_{pn})_{k\bar{k}'}. \quad (2.61)$$

For a nonrotating nucleus with $\omega=0$, then $t_{pn}^{(-)}=0$. For a rotating nucleus with $\omega \neq 0$, then $t_{pn}^{(-)} \neq 0$. In a rotating nucleus, Eq. (2.20) shows that if there are only np pairs and not $p\bar{p}$ pairs, then $t_{K\bar{K}'}=0$; however, Eq. (2.61) shows that $t_{k\bar{k}'} \neq 0$. This demonstrates that the $|K\rangle$, $|\bar{K}\rangle$ basis reduces the dimension of t by a factor of 2, compared to the $|k\rangle$, $|\bar{k}\rangle$ basis, for a rotating nucleus. The wave function in Eq. (2.51) shows that the neutron and proton in a given pair occupy

identical space-spin orbitals, i.e., $np(T=0)$ pairs. It is then interesting to find that $t_{k_p, \bar{k}'_n} \neq 0$ in a rotating nucleus. For a nonrotating nucleus, t would connect the $|k\rangle$ state and $|\bar{k}'\rangle$ state only if the neutron orbital were the time reverse of the proton orbital in the same pair, i.e., if there were $n\bar{p}(T=0)$ pairs rather than $np(T=0)$ pairs. It is also interesting to note that in a rotating nucleus $np(T=0)$ pairs give a t_{k_p, \bar{k}'_n} which is real; whereas in a nonrotating nucleus, the $n\bar{p}(T=0)$ pairs give a t_{k_p, \bar{k}'_n} which is imaginary [1]. The pair potential Δ separates into time-reversal even and odd components in the same manner as t , so that

$$\Delta_{pn}^{(\pm)} = \frac{1}{2} (\Delta_{pn} \pm \Delta_{\bar{p}\bar{n}}). \quad (2.62)$$

Also, one can substitute Δ for t in Eqs. (2.59)–(2.61).

D. Limiting case: $n\hat{n}$ and $p\hat{p}$ pairs

For a $N=Z$ =even nucleus, consider the case where there are neutron-neutron pairs and proton-proton pairs, but no neutron-proton pairs. This is accomplished by choosing $V_1=0$ and $V_2 \neq 0$ in the initial trial wave function. Then the final self-consistent wave function will have the same properties. Then the density matrix ρ of Eqs. (2.18) and (2.19) reduces to

$$\rho_{pp} = \rho_{nn} = \hat{V}_2^\dagger \hat{V}_2, \quad (2.63)$$

$$\rho_{\bar{p}\bar{p}} = \rho_{\bar{n}\bar{n}} = V_2^\dagger V_2. \quad (2.64)$$

The only nonzero components of the pairing tensor are $t_{p\bar{p}}$ and $t_{n\bar{n}}$, given by Eqs. (2.22) and (2.25).

The analysis of neutron-neutron pairs and proton-proton pairs in rotating nuclei, using the $|K\rangle, |\bar{K}\rangle$ basis states, was given in Refs. [18,19]. The result is that the HFB quasiparticle vacuum has the canonical representation

$$|\Phi_0\rangle = \prod_{\alpha>0} (u_\alpha + v_\alpha C_{ap}^\dagger C_{\alpha p}^\dagger)(u_\alpha - v_\alpha C_{an}^\dagger C_{\alpha n}^\dagger)|0\rangle, \quad (2.65)$$

where $u_\alpha^2 + v_\alpha^2 = 1$, and the canonical orbitals $|\alpha\rangle$ and $|\hat{\alpha}\rangle$ are given by Eqs. (2.39) and (2.43). It should be remembered that this is a spin-dependent state, where the orbitals and their occupation probabilities depend upon the rotational frequency ω . The nonzero elements of the density matrix are $\rho_{ap,ap} = \rho_{an,an} = \rho_{\hat{a}p,\hat{a}p} = \rho_{\hat{a}n,\hat{a}n} = v_\alpha^2$. The density matrix ρ is fourfold degenerate, even though the time-reversal symmetry is broken in the density matrix, with $\rho_{pp} \neq \rho_{\bar{p}\bar{p}}$. The nonzero elements of the pairing tensor are $t_{ap,\hat{a}p} = -t_{an,\hat{a}n} = u_\alpha v_\alpha$. For a rotating nucleus where $\omega \neq 0$, the time-reversal symmetry is broken, so that $|\hat{\alpha}\rangle \neq |\bar{\alpha}\rangle$. For a nonrotating nucleus where $\omega = 0$, the time-reversal symmetry is restored, so that $|\hat{\alpha}\rangle = |\bar{\alpha}\rangle$. Then the wave function simplifies to

$$|\Phi_0\rangle = \prod_{\alpha>0} (u_\alpha + v_\alpha C_{ap}^\dagger C_{\alpha p}^\dagger)(u_\alpha - v_\alpha C_{an}^\dagger C_{\alpha n}^\dagger)|0\rangle. \quad (2.66)$$

Because states (2.52) and (2.66) have different pair potentials Δ , self-consistency then leads to different HFB density matrices ρ . Therefore states (2.52) and (2.66) have different orbitals $|\alpha\rangle$ and different occupation probabilities v_α^2 . The time-reversal even and odd components of ρ , t , h , and Δ are given in Ref. [19].

E. Angular momentum and isospin of Cooper pairs

Each Cooper pair has an angular momentum J and isospin T . The HFB calculation provides the components of the pair potential $\Delta_{j_1 m_1 \tau_1, j_2 m_2 \tau_2}$ where τ is n or p . The pair potential can then be expressed in terms of the spin and isospin of the pair

$$\Delta_{j_1 j_2 J M T T_z} = \sum_{m_1 m_2 \tau_1 \tau_2} \langle j_1 m_1 j_2 m_2 | J M \rangle \times \langle \frac{1}{2} \tau_1 \frac{1}{2} \tau_2 | T T_z \rangle \Delta_{j_1 m_1 \tau_1, j_2 m_2 \tau_2}. \quad (2.67)$$

The strength of the pair potential for $J M T T_z$ is defined as

$$\Delta_{J M T T_z} = \sum_{j_1 \leq j_2} |\Delta_{j_1 j_2 J M T T_z}|. \quad (2.68)$$

The total strength of the pair potential for $J T$ is defined as

$$\Delta_{J T} = \left[\sum_{M T_z} |\Delta_{J M T T_z}|^2 \right]^{1/2}. \quad (2.69)$$

The pair potential has a time-reversal even component $\Delta^{(+)}$ and a time-reversal odd component $\Delta^{(-)}$, where $\Delta = \Delta^{(+)} + \Delta^{(-)}$. Consider the case of $n\hat{n}$ pairs and $p\hat{p}$ pairs, as in Eq. (2.65). Then $\Delta^{(+)}$ has M =even and $\Delta^{(-)}$ has M =odd. Also Δ has M =even if $\omega=0$ and Δ has M =even and odd if $\omega \neq 0$. Next consider the case of $np(T=0)$ pairs, as in Eq. (2.51). Then $\Delta^{(+)}$ has M =odd and $\Delta^{(-)}$ has M =even. Also Δ has M =odd if $\omega=0$ and Δ has M =even and odd if $\omega \neq 0$.

III. HFB CALCULATIONS

The model space includes the $2p_{1/2}$, $2p_{3/2}$, $1f_{5/2}$, and $1g_{9/2}$ shells. There is a closed core of $^{56}_{28}\text{Ni}$. For ^{80}Zr the maximum spin permitted by this model space is $38\hbar$. This model space was used in shell model Monte Carlo calculations for ^{74}Rb [6] and in HFB calculations for Sr, Zr, and Mo isotopes [22]. The Hamiltonian H contains an effective interaction calculated by T. Kuo from the Paris potential. This effective interaction was used in the ^{74}Rb calculation [6]. H also contains single-nucleon energies e_j , which are taken from Table II in Ref. [22], which extracts e_j from experimental spectra in this mass region. The Coulomb interaction is not included. Further details regarding H are given in Refs. [16,17]. Axial and triaxial deformations are included. The pair potential Δ includes components with isospin $T=0,1$ and angular momentum $J=0,1,2,3,4,5,6,7,8,9$. Self-consistency is obtained in both h and Δ for each nuclear spin I . [This means that Eq. (2.30) is solved in the usual iterative

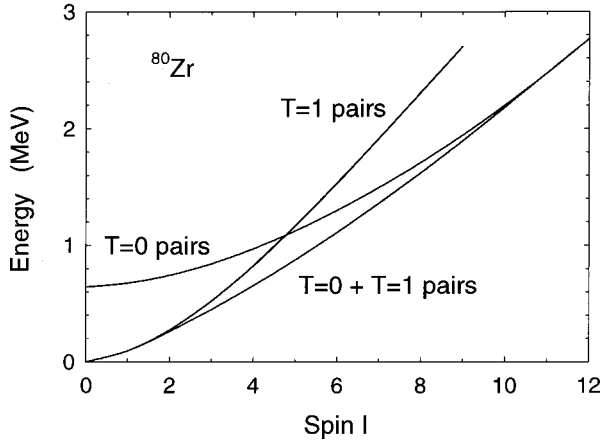


FIG. 1. Energies of the rotational bands versus the spin I .

procedure. On each iteration h and Δ are calculated from the density matrix ρ and the pairing tensor t , respectively; then ρ and t are calculated from the eigenvectors (U_j, V_j) in Eq. (2.30). The iterations continue until h and Δ do not vary on successive iterations.] Because the model space contains only one value of the radial quantum number n for each lj , there is no self-consistency in the radial coordinate. Number parity is conserved on each iteration.

A. Rotational energies

As described in Sec. II A, the ground state has $n\bar{n}$ pairs and $p\bar{p}$ pairs. These are $T=1$ pairs. It has the canonical representation given in Eq. (2.66). The HFB equation (2.30) is used to rotate the $T=1$ pair state (2.66). This generates a rotational band with $T=1$ ($n\hat{n}$ and $p\hat{p}$) pairs. The calculated energies of the $I^\pi=2^+$ and 4^+ states are 0.274 and 0.826 MeV, respectively. (This calculation has no parameters available to adjust the energies of rotational states.) The corresponding experimental energies are 0.290 and 0.828 MeV [23,24]. For each spin I , the HFB state has the spin-dependent canonical form given in Eq. (2.65).

Section II A also describes the HFB excited state at $E = 0.645$ MeV, which has $np(T=0)$ pairs and $\bar{n}\bar{p}(T=0)$ pairs. This state has the canonical representation given in Eq. (2.52). The HFB equation (2.30) is used to rotate the $T=0$ pair state (2.52). This generates a rotational band with $T=0$ (np and $\hat{n}\hat{p}$) pairs. For each spin I , the HFB state has the spin-dependent canonical form given in Eq. (2.51).

The energies of the $T=1$ pair band and the $T=0$ pair band are shown in Fig. 1. The two bands cross at spin $I \approx 5\hbar$. Consequently the yrast line obtained from these two crossing bands has a ‘‘phase transition’’ at $I \approx 5\hbar$. The yrast states for $I \leq 4\hbar$ have $T=1$ Cooper pairs, whereas the yrast states for $I \geq 6\hbar$ have $T=0$ Cooper pairs. If this HFB calculation had been performed with only neutron-neutron pairing and proton-proton pairing, and the neutron-proton pairing had been omitted, then the $T=0$ pair band would not have been found, and the yrast line would coincide with the $T=1$ pair band at all spins. No phase transition would have been predicted. The energies of both bands have been calcu-

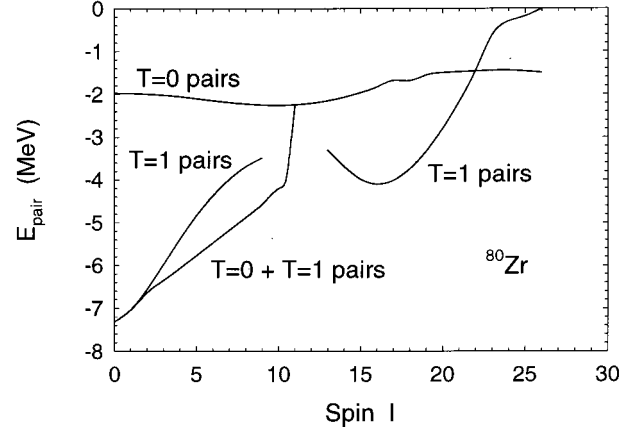


FIG. 2. Pair correlation energy E_{pair} for the $T=0$ pair band, the $T=1$ pair band, and the $T=0+T=1$ pair band.

lated up to spin $I=26\hbar$. At high spins, the $T=1$ pair band has a higher energy than the $T=0$ pair band. As will be shown below, the $T=1$ pair band has a large backbend between spins $I=8$ and $I=14$. The spin $I=10,12$ states have not been found for this band. (This sometimes occurs for HFB states in the middle of a backbend, as they may be unstable.)

In the band crossing region is there a lower energy HFB state which contains both $T=1$ pairs and $T=0$ pairs in the same HFB wave function? (Such wave functions have been found for the ground states of ^{84}Mo and ^{88}Ru [16,17].) The HFB equation is used to obtain a band which contains both $T=1$ ($n\hat{n}, p\hat{p}$) pairs and $T=0$ ($np, \hat{n}\hat{p}$) pairs. This band is shown in Fig. 1. This band forms an envelope to the $T=1$ pair band and the $T=0$ pair band. It joins smoothly to the $T=1$ pair band at $I=0$ and to the $T=0$ pair band at high spins. For spins near $5\hbar$, both $T=1$ pairs and $T=0$ pairs are contained in the same HFB wave function for a given spin I . At $I=0$ the HFB state for the envelope is exactly the same as the HFB state in the $T=1$ pair band, and it contains only $T=1$ pairs. At $I=11$ the HFB state of the envelope is almost the same as the HFB state of the $T=0$ pair band, and it contains primarily $T=0$ pairs. The envelope band provides an yrast line which is much smoother than the yrast line given by the two crossing bands. For the $T=0+T=1$ pair band, the energy of the $I^\pi=4^+$ state is below the experimental energy.

Figure 2 shows the pairing energy, $E_{pair} = \text{Tr}[\frac{1}{2}\Delta t^\dagger]$. The $T=1$ pair band has a large (negative) pairing energy at spin $I=0$. However, as the spin increases, this band rapidly loses its pairing energy, which vanishes at $I=26$. In contrast, the $T=0$ pair band has a pairing energy which is approximately constant for increasing spin. (The pairing energy actually increases with I at low spins, i.e., becomes more negative.) The $T=0+T=1$ pair band loses its pairing energy less rapidly than the $T=1$ pair band.

Why does $E_{pair}(I)$ behave so differently for the $T=1$ pair band and the $T=0$ pair band? First consider the $T=1$ pair band. At spin $I=0$ the two nucleons in each Cooper pair are in time-reversed orbitals, where m_z is a good quantum num-

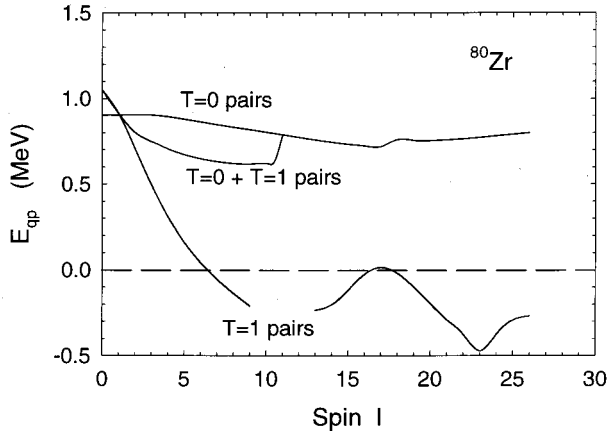


FIG. 3. Lowest quasiparticle energy E_1 for the $T=0$ pair band, the $T=1$ pair band, and the $T=0+T=1$ pair band.

ber, and the first nucleon has $+m$ while the second has $-m$. When this state is rotated, the Coriolis force has an opposite effect on the angular momentum vectors of the two nucleons, thereby breaking the time-reversal symmetry, and breaking the pair bond. This is the Coriolis antipairing (CAP) effect, which causes the rapid loss of pairing energy as the spin I increases [25]. For $T=1$ pairs the isospin state is symmetric, so the space-spin state must be antisymmetric. This permits $J=0$ pairs, which is the strongest pair mode. The rotation breaks these $J=0$ pairs in order to realign the nucleon spins along the x rotation axis and generate the nuclear spin I .

Next consider the $T=0$ pair band. At spin $I=0$ the neutron and proton in each Cooper pair occupy identical space-spin orbitals, where m_z is a good quantum number. When this state is rotated, the Coriolis force has exactly the same effect on the angular momentum vectors of the two nucleons. The two spin vectors can be gradually rotated towards the x rotation axis, and at each spin I the neutron and proton in a pair will have the same space-spin wave function, thereby maintaining maximum spatial overlap. The pair is not broken by the rotation. There is no CAP effect for these $T=0$ pairs. Therefore the pairing energy is approximately constant for increasing spin I . For $T=0$ pairs the isospin state is antisymmetric, so the space-spin state is symmetric. This forbids $J=0$ pairs. Each pair has at least $J=1$. Then each pair can contribute to the nuclear spin I by gradually realigning its spin J from the z axis to the x rotation axis, without breaking the pair.

B. Quasiparticle energies

The Coriolis force can cause the lowest quasiparticle energy E_1 to vanish at a critical angular velocity ω_c , even though the pair field Δ is not zero [26]. For $\omega > \omega_c$, it is necessary to have negative values of E_1 in order to conserve the number parity [27]. One must also ensure that the two quasiparticle excitation energy $E_1 + E_2$ remains non-negative. The lowest quasiparticle energy E_1 is shown in Fig. 3. For the $T=1$ pair band, E_1 decreases rapidly with spin and changes sign at $I \approx 6$, even though the pairing en-

ergy does not vanish until $I=26$. In sharp contrast, for the $T=0$ pair band, E_1 is approximately constant with spin, and it does not change sign. This is another signal of the radically different manner in which $T=1$ pairs and $T=0$ pairs respond to rotation. For the $T=0+T=1$ pair band, E_1 initially follows the decrease of the $T=1$ pair band, but quickly levels off and then joins the path of the $T=0$ pair band, so that E_1 is never close to zero. So for $I \approx 6$, where this band contains both $T=0$ pairs and $T=1$ pairs at the same spin I , the presence of the $T=0$ pairs prevents E_1 from decreasing very much.

C. Pair potential

The pair potential has a matrix representation Δ_{ij} . It is therefore convenient to define various ways of characterizing the average properties of this matrix. Each pair mode is described by a submatrix of Δ . Consider the average of the ‘‘diagonal’’ elements for each submatrix of Δ

$$\bar{\Delta}_{pp}^{(+)} = \bar{\Delta}_{nn}^{(+)} = \frac{1}{M} \sum_{K=1}^M |\Delta_{Kp, \bar{K}p}^{(+)}| = \frac{1}{M} \sum_{k=1}^M |\Delta_{kp, \bar{k}p}|, \quad (3.1)$$

$$\bar{\Delta}_{pp}^{(-)} = \bar{\Delta}_{nn}^{(-)} = \frac{1}{M} \sum_{K=1}^M |\Delta_{Kp, \bar{K}p}^{(-)}| = \frac{1}{M} \sum_{k=1}^M |\Delta_{kp, kp}| = 0, \quad (3.2)$$

$$\bar{\Delta}_{pn}^{(+)} = \frac{1}{M} \sum_{K=1}^M |\Delta_{Kp, Kn}^{(+)}| = \frac{1}{M} \sum_{k=1}^M |\Delta_{kp, kn}|, \quad (3.3)$$

$$\bar{\Delta}_{pn}^{(-)} = \frac{1}{M} \sum_{K=1}^M |\Delta_{Kp, Kn}^{(-)}| = \frac{1}{M} \sum_{k=1}^M |\Delta_{kp, \bar{k}n}|. \quad (3.4)$$

The last sum in each of these equations considers a submatrix of Δ in the $|k\rangle, |\bar{k}\rangle$ basis. They are related to the corresponding time-reversal even or odd component of Δ expressed in the $|K\rangle, |\bar{K}\rangle$ basis. The 0 at the end of Eq. (3.2) occurs because $\Delta_{kp, kp} = 0$ (Δ is antisymmetric), although $\Delta_{kp, k'p} \neq 0$ and $\Delta_{pp}^{(-)} \neq 0$ for $\omega \neq 0$. A single average value of Δ is defined as

$$\bar{\Delta} = \frac{1}{M} \sum_{k=1}^M [|\Delta_{kp, \bar{k}p}|^2 + |\Delta_{kp, \bar{k}n}|^2 + |\Delta_{kp, kn}|^2]^{1/2}. \quad (3.5)$$

Figure 4 shows $\bar{\Delta}$. For the $T=1$ pair band, $\bar{\Delta}$ decreases with spin, and vanishes at spin $I=26$. For the $T=0$ pair band, $\bar{\Delta}$ is approximately constant with spin, up to $I=26$. There is a small bump at $I=18$, which will be explained below. At $I=0$ the value of $\bar{\Delta}$ is larger for the $T=1$ pair band than for the $T=0$ pair band. This is primarily because for $I=0$ with $T=0$ pairs, only certain orbitals near the Fermi energy participate in the pairing (as described below), so that the average $\bar{\Delta}$ includes some large terms and some zero terms, whereas for $T=1$ pairs more orbitals participate in the pairing. For the $T=0+T=1$ pair band, $\bar{\Delta}$ initially follows the $T=1$ pair band; then at $I \approx 5$, $\bar{\Delta}$ is larger than for the $T=1$

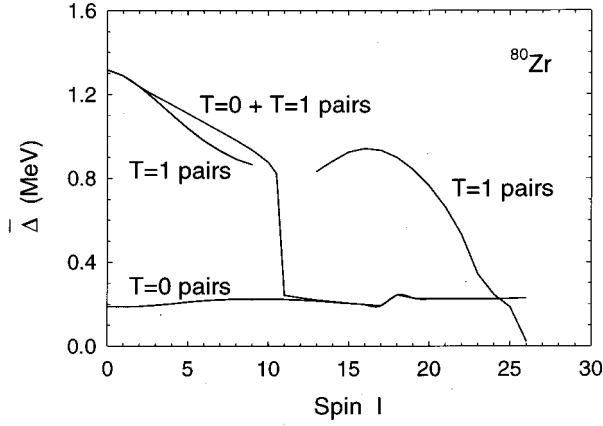


FIG. 4. Average pair potential $\bar{\Delta}$ for the $T=0$ pair band, the $T=1$ pair band, and the $T=0+T=1$ pair band.

pair band because both $T=0$ and $T=1$ pairs coexist; and finally for $I>10$, $\bar{\Delta}$ follows the $T=0$ pair band.

The discussion above considers the matrix representation of Δ in the spherical basis $|k\rangle$. Alternatively, one can express Δ in the canonical basis $|\alpha\rangle$ described in Sec. II C 1. Then the average value of the “diagonal” elements for each submatrix of Δ are defined by

$$\bar{\Delta}_{pp} = \bar{\Delta}_{nn} = \frac{1}{M} \sum_{\alpha=1}^M |\Delta_{\alpha p, \hat{\alpha} p}|, \quad (3.6)$$

$$\bar{\Delta}_{pn} = \frac{1}{2M} \sum_{\alpha=1}^{2M} |\Delta_{\alpha p, \alpha n}|, \quad (3.7)$$

where the sum in Eq. (3.7) includes the terms where $|\alpha\rangle = |\hat{\alpha}\rangle$. A single average value of Δ is defined as

$$\bar{\Delta} = \frac{1}{2M} \sum_{\alpha=1}^{2M} [|\Delta_{\alpha p, \hat{\alpha} p}|^2 + |\Delta_{\alpha p, \alpha n}|^2]^{1/2}. \quad (3.8)$$

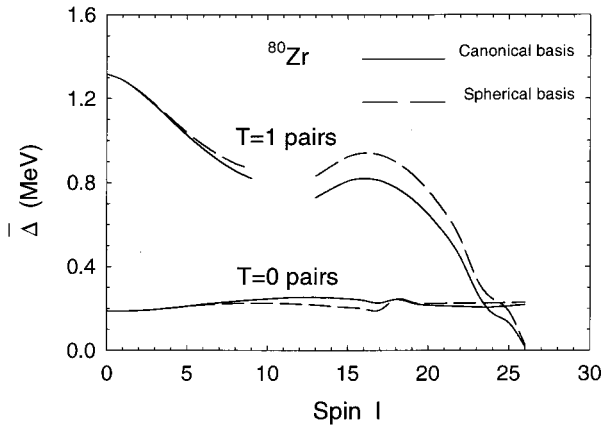


FIG. 5. Average pair potential $\bar{\Delta}$ for the $T=0$ pair band and the $T=1$ pair band. The canonical basis $|\alpha\rangle$ is compared to the spherical basis $|k\rangle$.

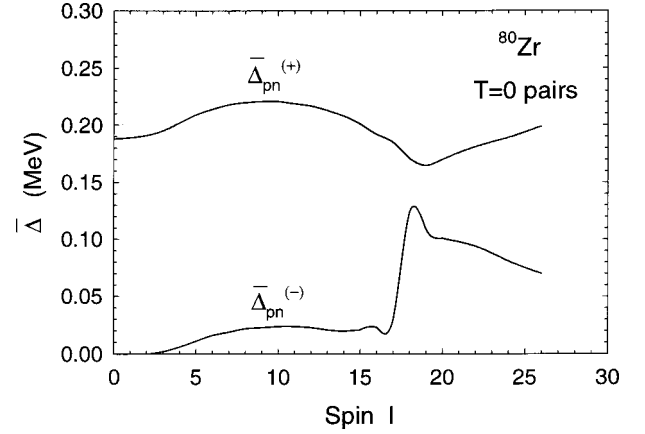


FIG. 6. Average time-reversal even and odd components of the pair potential $\bar{\Delta}_{pn}^{(\pm)}$ for the $T=0$ pair band.

Recall that in the canonical basis $\Delta_{\alpha p, \hat{\alpha} n} = 0$, so this term does not contribute. Figure 5 shows $\bar{\Delta}$ for the canonical basis $|\alpha\rangle$ and compares it to the values for the spherical basis $|k\rangle$. The two bases give similar results for $\bar{\Delta}$.

Next we compare the time-reversal even and time-reversal odd components of the pair potential. The average values of these components are defined in Eqs. (3.1)–(3.4). Figure 6 shows $\bar{\Delta}_{pn}^{(+)}$ and $\bar{\Delta}_{pn}^{(-)}$ for the $T=0$ pair band. At spin $I=0$ the pair potential is time-reversal invariant, so that $\bar{\Delta}_{pn}^{(-)} = 0$. However, as the spin increases, the time-reversal symmetry is broken, so that $\bar{\Delta}_{pn}^{(-)}$ increases. At $I \approx 18$ there is a sudden increase in $\bar{\Delta}_{pn}^{(-)}$. Then $\bar{\Delta}_{pn}^{(-)}$ is almost as large as $\bar{\Delta}_{pn}^{(+)}$, and it would clearly be impermissible to neglect the time-reversal violation of the pair potential. This sudden increase in $\bar{\Delta}_{pn}^{(-)}$ is reflected in the small bump at $I \approx 18$ in the $T=0$ curve in Fig. 4.

Figure 7 shows $\bar{\Delta}_{pn}^{(+)}$, $\bar{\Delta}_{pn}^{(-)}$, and $\bar{\Delta}_{pp}^{(+)}$ for the $T=0+T=1$ pair band. At spin $I=0$ only $\bar{\Delta}_{pp}^{(+)}$ is nonzero, so there are only pp and nn pairs. As the spin increases, $\bar{\Delta}_{pp}^{(+)}$ de-

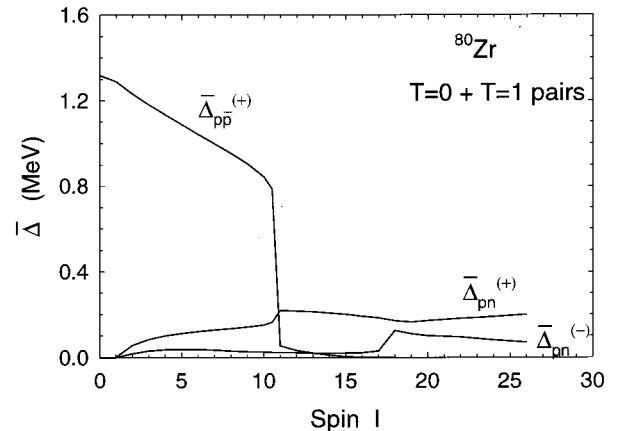


FIG. 7. Average time-reversal even and odd components of the pair potential $\bar{\Delta}_{pn}^{(\pm)}$ and $\bar{\Delta}_{pp}^{(\pm)}$ for the $T=0+T=1$ pair band.

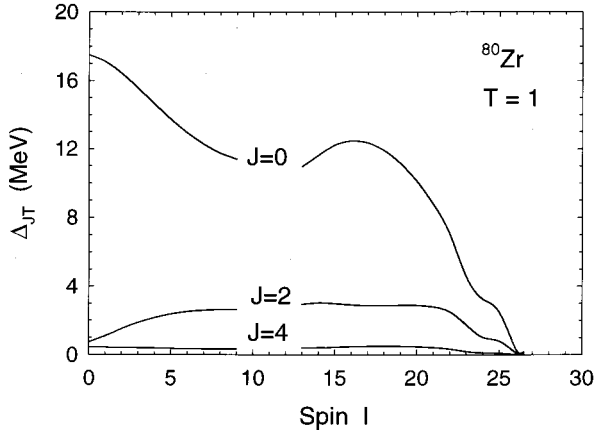


FIG. 8. Angular momentum components of the pair potential $\Delta_{J,T=1}$ for the $T=1$ pair band.

creases and $\bar{\Delta}_{pn}^{(\pm)}$ increases. This figure shows that for the spin interval $I=2-10$, there are np pairs as well as $p\hat{p}$ and $n\hat{n}$ pairs coexisting at each spin. At $I \approx 10$, $\bar{\Delta}_{pp}^{(\pm)}$ suddenly becomes very small, and it vanishes at $I \approx 16$.

Each Cooper pair has an angular momentum J and isospin T . The pair potential has spin and isospin components Δ_{JT} , given by Eq. (2.69). Figure 8 shows Δ_{JT} for the $T=1$ pair band. As expected, at spin $I=0$ the monopole ($J=0$) pairs dominate, while the $J=2$ and $J=4$ pairs are much less important. However, as the spin I increases, the $J=0$ pairs decrease, whereas the $J=2$ and $J=4$ pairs increase. However, at all spins I the monopole pairing is the largest. At $I=26$, the $T=1$ pairs vanish, simultaneously for all J .

The pair potential Δ_{JT} for the $T=0$ pair band is shown in Fig. 9. The conventional wisdom for $T=0$ pairs is that the most important value of J for a pair is $J=1$; although it is sometimes stated that the dominant value is either $J=1$ or $J=J_{max}=2j$, where j is the nucleon spin. Figure 9 shows that neither of these typical assumptions is correct for ^{80}Zr . At spin $I=0$ there are no $J=1$ pairs and no $J=3$ pairs. As the spin I increases, $J=1$ and $J=3$ pairs emerge, but their

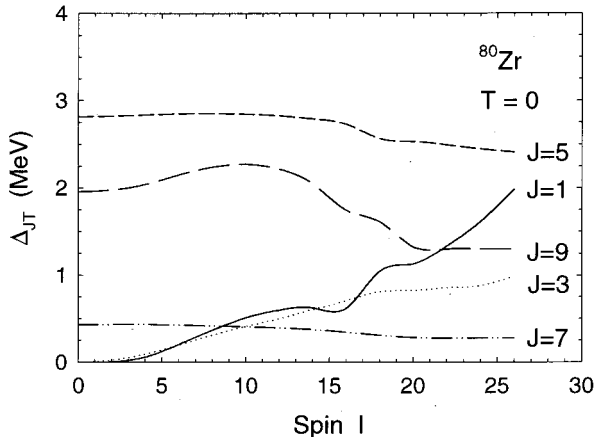


FIG. 9. Angular momentum components of the pair potential $\Delta_{J,T=0}$ for the $T=0$ pair band.

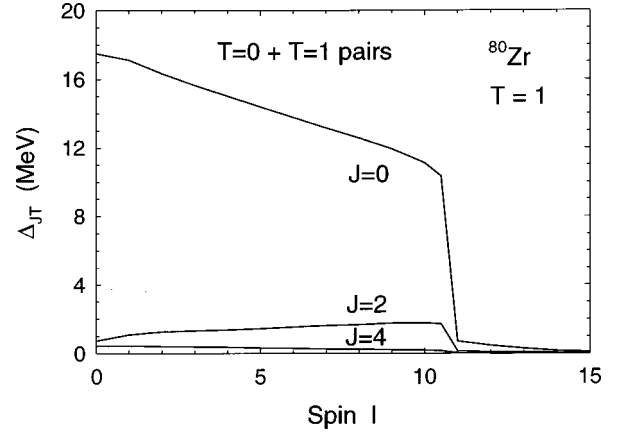


FIG. 10. Angular momentum components of the pair potential $\Delta_{J,T=1}$ for the $T=0+T=1$ pair band.

strength remains relatively weak for spins $I \leq 10$. It is only at spins $I \geq 20$ that the $J=1$ pairs become strong. For our model space the $1g_{9/2}$ shell provides $J_{max}=9$. There is a large component of $J=9$ pairs for all I . The $J=7$ pairs exist at all I , but are less important. The surprise which upsets the conventional wisdom for $T=0$ pairs is that the greatest strength at all spins I comes from the $J=5$ pairs.

Why are the $J=5$ pairs the most important $T=0$ pairs? The reason is as follows. The orbitals which make the largest contribution to the pair potential Δ are the orbitals which are closest to the Fermi energy. For the $T=0$ pair band at spin $I=0$, these are the n and p $1f_{5/2}$ $m = \pm 5/2$ orbitals, with occupation probability $v^2=0.35$, and the n and p $1g_{9/2}$ $m = \pm 5/2$ orbitals, with $v^2=0.65$. This identifies the four Cooper pairs which are closest to the Fermi energy. (For spin $I=0$, all other pairs have $v^2=0$ or 1, and do not contribute to Δ .) Because the neutron and proton in each pair have the same space-spin orbital, each of these four pairs has $M = \pm 5$. Therefore these pairs have J restricted to $J=5,7,9$, whereas $J=1$ and $J=3$ are forbidden. All four of these $f_{5/2}$ pairs and $g_{9/2}$ pairs can contribute to the $J=5$ pair mode, but only the two $g_{9/2}$ pairs can contribute to the $J=7,9$ pair modes. The result is that the $J=5$ pair mode is dominant. Of course this result occurs because of the position of the Fermi energy in ^{80}Zr , and the result could be completely different in other $N=Z$ nuclei.

Finally consider the $T=0+T=1$ pair band. Figure 10 shows $\Delta_{J,T=1}$ and Fig. 11 shows $\Delta_{J,T=0}$ for this band. Observe that for the spin interval $I=2-10$ there are both $T=0$ pairs and $T=1$ pairs at each spin I coexisting in the same wave function. For the $T=1$ pairs, the monopole ($J=0$) pairs are largest. The $J=0$ pairs decrease with I , whereas the $J=2$ and $J=4$ pairs increase with I . At $I \approx 11$, the $T=1$ pairs suddenly become very weak, simultaneously for all J . There are no $T=0$ pairs at $I=0$. However, at $I=2$ the $T=0$ pairs emerge, with increasing strength as I increases. For $I > 10$ the $T=0$ pairs remain large, while the $T=1$ pairs are negligible. For the $T=0$ pairs, $J=9$ has the greatest strength for $I \leq 10$, whereas $J=5$ is largest for $I > 10$. It is interesting to compare $\Delta_{J,T=0}$ for the $T=0$ pair band (Fig. 9) and $\Delta_{J,T=0}$ for the $T=0+T=1$ pair band (Fig.

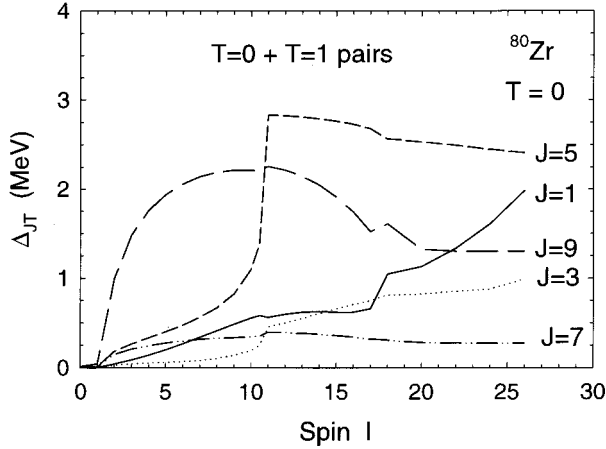


FIG. 11. Angular momentum components of the pair potential $\Delta_{J,T=0}$ for the $T=0+T=1$ pair band.

11). For $I \leq 10$ the $T=0$ pair band has $J=5$ largest, whereas the $T=0+T=1$ pair band has $J=9$ largest with $J=5$ much smaller. The presence of the $T=1$ pairs in the $T=0+T=1$ pair band has caused a reduction in $\Delta_{J=5, T=0}$. The mechanism for $T=1$ pairs to affect $T=0$ pairs is through the orbital occupation probabilities. Each orbital can gain occupation probability through its participation in a $T=0$ pair and through its participation in a $T=1$ pair. Therefore for each orbital $|\alpha\rangle$ the occupation is $v_\alpha^2 = v_{\alpha, T=0}^2 + v_{\alpha, T=1}^2$. Since $0 \leq v_\alpha^2 \leq 1$, and since the sum of the occupations v_α^2 must be constrained to equal the particle number, it follows that an increase in $v_{\alpha, T=1}^2$ might cause a decrease in $v_{\alpha, T=0}^2$. This mechanism can divert occupation probability from $T=0$ pairs to $T=1$ pairs for the $1f_{5/2} m = \pm 5/2$ orbitals, thereby causing a decrease in $\Delta_{J=5, T=0}$.

D. Moment of inertia

The static moment of inertia is $\mathcal{I} = \langle J_x \rangle / \omega$, where $\langle J_x \rangle = [I(I+1)]^{1/2}$. It is shown in Fig. 12. The $T=1$ pair band

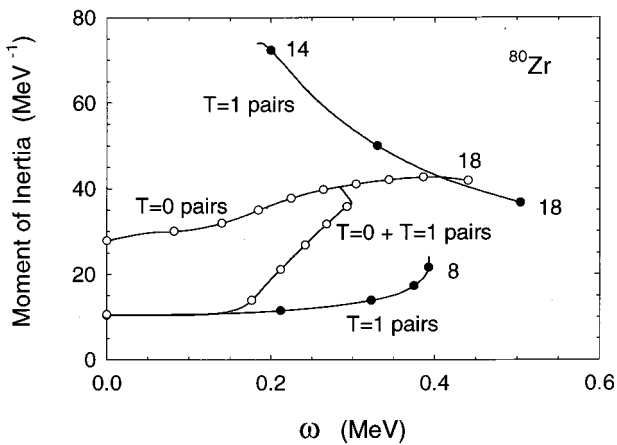


FIG. 12. Static moment of inertia \mathcal{I} versus rotational frequency ω for the $T=0$ pair band, the $T=1$ pair band, and the $T=0+T=1$ pair band.

has a large backbend between spins $I=8$ and $I=14$. The spin $I=10,12$ states have not been found for this band. (This sometimes occurs for HFB states in the middle of a backbend, as they may be unstable.) In contrast the $T=0$ pair band has no backbend, but only a slow increase in the moment of inertia up to $I=16$, followed by a considerable decrease at higher spins. This demonstrates how $T=1$ pairs and $T=0$ pairs respond to rotation in a significantly different manner. The $T=0+T=1$ pair band coincides with the $T=1$ pair band at $I=0$ and joins the $T=0$ pair band at $I=11$. It has a small backbend at $I \approx 11$. If $T=0$ pairing had been omitted in this calculation, then the yrast line would simply follow the $T=1$ pair band for all I , and the yrast line would have a large backbend between spins 8 and 14. It should also be observed that if a different Hamiltonian H would produce band-head energies so that $E_{T=0}(I=0) < E_{T=1}(I=0)$, then the $T=0$ pair band would be lower in energy than the $T=1$ pair band for all spins I . Then the yrast line would coincide with the $T=0$ pair band, and show no backbend.

At spin $I=0$ the moment of inertia for $T=0$ pairs is much larger than for $T=1$ pairs. The essential reason is obtained from the Belyaev formula [28] for \mathcal{I}_{BCS} at $I=0$

$$\mathcal{I}_{BCS} = 2 \sum_{\alpha\beta>0} \frac{|\langle \alpha | J_x | \beta \rangle|^2}{E_\alpha + E_\beta} (u_\alpha v_\beta - u_\beta v_\alpha)^2. \quad (3.9)$$

Isospin generalized BCS calculations at $I=0$ give $\mathcal{I}_{BCS}(T=0)/\mathcal{I}_{BCS}(T=1) = 2.04$. The essential reason why the moment of inertia is larger for $T=0$ pairs than for $T=1$ pairs comes from the factor $f_{\alpha\beta} = (u_\alpha v_\beta - u_\beta v_\alpha)^2$. Let $\alpha = m_z$ designate the orbital $g_{9/2} m_z$. Then the terms in \mathcal{I}_{BCS} with $(\alpha, \beta) = (3/2, 5/2)$ and $(5/2, 7/2)$ (and their time reverses) account for 84% of $\mathcal{I}_{BCS}(T=0)$ and 76% of $\mathcal{I}_{BCS}(T=1)$. The ratio $f_{\alpha\beta}(T=0)/f_{\alpha\beta}(T=1)$ is 2.41 for $(\alpha, \beta) = (3/2, 5/2)$ and 1.89 for $(\alpha, \beta) = (5/2, 7/2)$, which accounts for the large value of $\mathcal{I}_{BCS}(T=0)$. These ratios of $f_{\alpha\beta}$ are large because for $T=1$ pairs, all orbitals participate in the pairing and have partial occupation probabilities v_α^2 , so $f_{\alpha\beta}$ is small; whereas for $T=0$ pairs at $I=0$, only the $m_z = \pm 5/2$ orbitals participate in the pairing, so that $v_{3/2}^2 = 1$ and $v_{7/2}^2 = 0$, and these $f_{\alpha\beta}$ are large. Whereas the factor $f_{\alpha\beta}$ greatly reduces \mathcal{I} for the $T=1$ pair superfluid (where $J=0$ is primary), this is not so for this $T=0$ pair superfluid (where $J>0$), so that $\mathcal{I}_{BCS}(T=0)/\mathcal{I}_{HF} = 0.99$. Rotating pairs with $J>0$ is different than rotating pairs with $J=0$.

E. Spin alignments

In this section we consider how rotating $T=1$ pairs and $T=0$ pairs generates the nuclear angular momentum. Figure 13 shows $\langle J_x \rangle = [I(I+1)]^{1/2}$, where

$$\langle J_x \rangle = \text{Tr}[J_x \rho] = 2 \sum_{\alpha} \langle \alpha | J_x | \alpha \rangle v_\alpha^2, \quad (3.10)$$

where $|\alpha\rangle$ are the canonical orbitals, the sum includes the terms with $|\alpha\rangle = |\hat{\alpha}\rangle$, and the factor of 2 indicates that neutrons and protons have identical orbitals and occupation

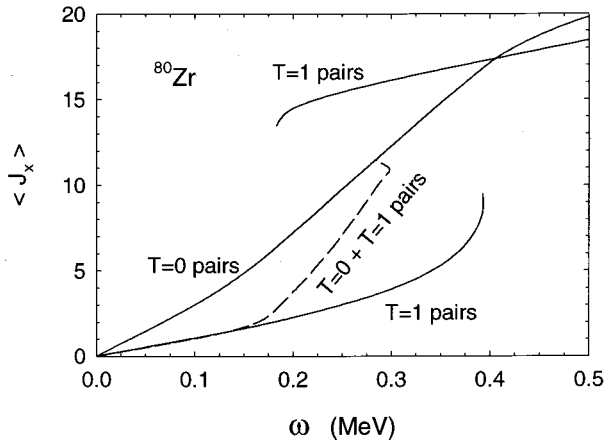


FIG. 13. Angular momentum $\langle J_x \rangle$ versus rotational frequency ω for the $T=0$ pair band, the $T=1$ pair band, and the $T=0+T=1$ pair band.

probabilities. For the $T=1$ pair band there is a large backbend with a sudden increase in the angular momentum. In contrast the $T=0$ pair band has a gradual increase in the spin with no backbend.

Which nucleons are responsible for generating the nuclear spin? Figure 14 shows the contributions to the nuclear spin generated by different shells for the $T=1$ pair band. The pf shells have a very small contribution to the spin. Almost all of the angular momentum originates from the $g_{9/2}$ shell. This figure also shows the contribution to $\langle J_x \rangle$ from two $g_{9/2}$ pairs, i.e., one $nn\hat{n}$ pair and one $pp\hat{p}$ pair, where the orbitals are canonical orbitals. Since the space-spin wave functions of the $nn\hat{n}$ pair are identical to those of the $pp\hat{p}$ pair, the two pairs have identical responses to rotation at each spin I . At $I=13$ the total $\langle J_x \rangle=13.49$ while these two pairs have $\langle J_x \rangle=15.35$. All of the other orbitals actually combine to have a negative contribution to the spin. The maximum $\langle J_x \rangle$ for one $g_{9/2}$ pair is $9/2+7/2=8$, so that the maximum spin for two pairs is 16. This suggests that at $I=13$ these two pairs have come close to their maximum possible spin alignment. At $I=0$ each pair has antiparallel nucleon spins aligned along the

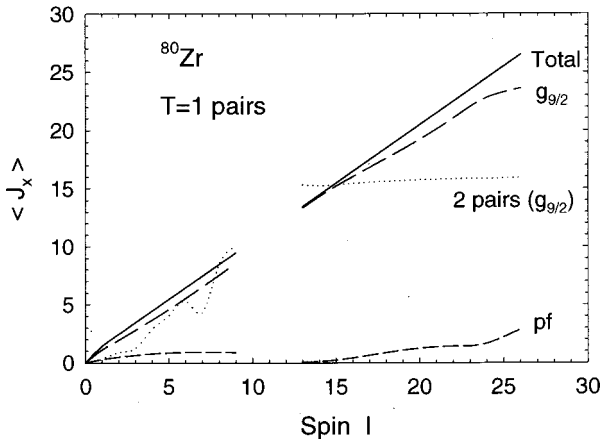


FIG. 14. Angular momentum contributions from different shells for the $T=1$ pair band.

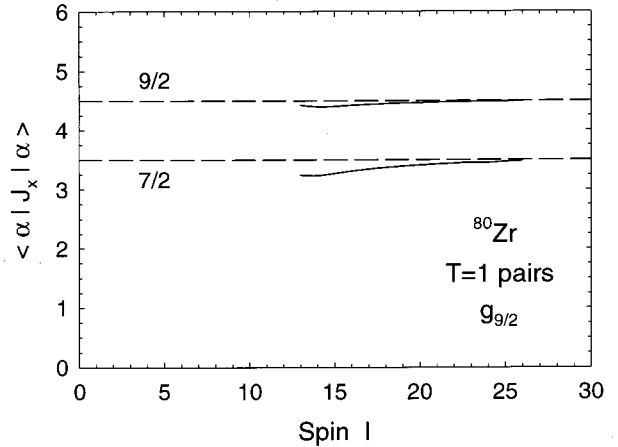


FIG. 15. Spin alignments for each orbital in the rotation aligned $g_{9/2}$ pairs for the $T=1$ pair band.

z deformation symmetry axis, whereas at $I=13$ each pair has almost parallel nucleon spins aligned along the x rotation axis. This is the rotational realignment effect [29].

This conjecture is confirmed by considering the spin alignment $\langle \alpha | J_x | \alpha \rangle$ for each $g_{9/2}$ neutron canonical orbital in the $nn\hat{n}$ pair, shown in Fig. 15. The proton spin alignments in the $pp\hat{p}$ pair are identical to the neutron spin alignments. At high spins these orbitals have spin alignments which are very close to the values for completely aligned $g_{9/2}$ orbitals. At $I=13$, the first orbital in a pair has a 98.5% overlap with the J_x eigenstate $|g_{9/2}m_x=9/2\rangle$, and the second orbital in a pair has a 94.3% overlap with the J_x eigenstate $|g_{9/2}m_x=7/2\rangle$. This confirms that in the backbend of the $T=1$ pair band, two $g_{9/2}$ neutrons and two $g_{9/2}$ protons are realigning their spins along the x rotation axis.

Now consider the spin alignments in the $T=0$ pair band. Figure 16 shows the contributions to the nuclear spin from different shells. The pf shells make a very small contribution to the spin. Almost all of the angular momentum comes from the $g_{9/2}$ shell. This figure shows the contribution to $\langle J_x \rangle$ from two $g_{9/2}$ np pairs, where the n and p in a specific pair have

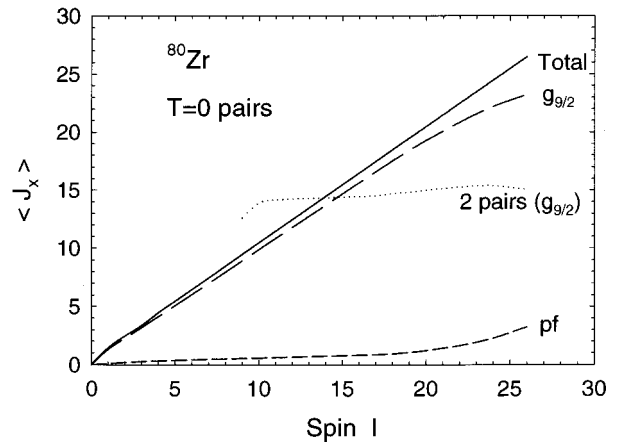


FIG. 16. Angular momentum contributions from different shells for the $T=0$ pair band.

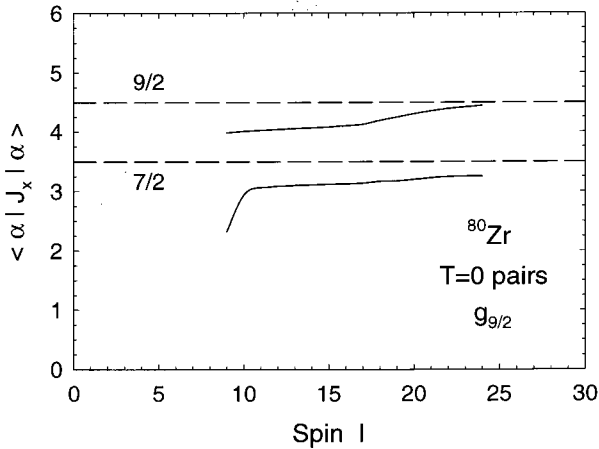


FIG. 17. Spin alignments for each orbital in the rotation aligned $g_{9/2}$ pairs for the $T=0$ pair band.

identical canonical orbitals. Therefore the n and p in a given pair respond to rotation in an identical manner. At $I=13$ the total $\langle J_x \rangle = 13.49$ while these two pairs have $\langle J_x \rangle = 14.32$. All of the other orbitals combine to have a negative contribution to the spin. At $I=13$ these two $T=0$ pairs have a spin alignment which is not far from the maximum possible value of 16, and only $1\hbar$ less than the spin of the $T=1$ pairs at $I=13$. At $I=0$ each pair has parallel nucleon spins aligned along the z deformation symmetry axis, whereas at $I=13$ each pair has parallel nucleon spins aligned along the x rotation axis. This is a rotational realignment effect.

The spin alignment $\langle \alpha | J_x | \alpha \rangle$ for the $g_{9/2}$ neutron canonical orbital in each of the two np pairs is shown in Fig. 17. The proton spin alignments are identical to the neutron spin alignments. At high spins these orbitals have spin alignments which are near the values for aligned $g_{9/2}$ orbitals. At $I=13$, the n and p orbitals in the first pair have a 90.5% overlap with the J_x eigenstate $|g_{9/2}m_x=9/2\rangle$, and the n and p orbitals in the second pair have a 90.4% overlap with the J_x eigenstate $|g_{9/2}m_x=7/2\rangle$. These orbitals are substantially, but not completely, aligned. This confirms that in the $T=0$ pair band, two $g_{9/2}$ neutrons and two $g_{9/2}$ protons are realigning their spins along the x rotation axis. However, the spin alignments in the $T=0$ pair band do not produce an upbend or backbend in the moment of inertia. It is sometimes stated that an energy spectrum without an upbend or backbend does not contain spin alignments. However, this analysis demonstrates that the absence of an upbend or backbend in the moment of inertia does not imply the absence of spin alignments for a $T=0$ pair band.

F. Delayed alignments

A new experiment on ^{80}Zr has identified states up to $I=12$ [30]. At low spins the experimental energies are very close to the HFB $T=1$ pair band, and at higher spins the experiment shows a slowly rising moment of inertia, with no backbend or upbend. Since ^{82}Zr and ^{84}Zr have upbends caused by $g_{9/2}$ alignments at spins below $I=12$ [31], the ^{80}Zr spectrum is anomalous, and has been characterized as a de-

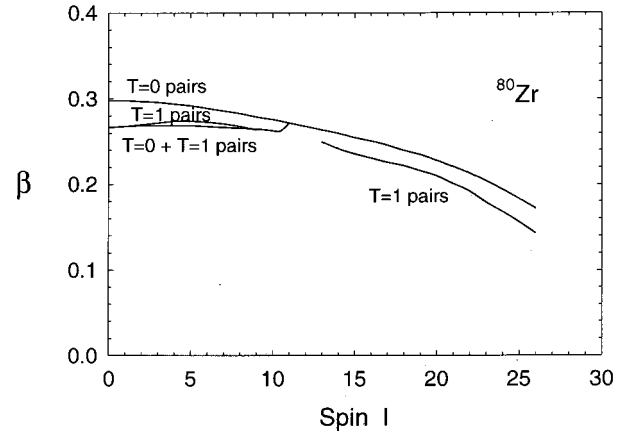


FIG. 18. Quadrupole deformation parameter β for the $T=0$ pair band, the $T=1$ pair band, and the $T=0+T=1$ pair band.

layed alignment. (Similar delayed alignments have been observed in the $N=Z$ nuclei ^{72}Kr and ^{76}Sr [32].) The HFB $T=1$ pair band and $T=0$ pair band were completed before I became aware of this ^{80}Zr experiment. The HFB yrast band ($T=0+T=1$ pair band) is not similar to the experimental band. Although this HFB calculation does not explain the ^{80}Zr experiment, it offers one ingredient of a possible explanation. It shows that for $T=0$ pairing in ^{80}Zr , there are $g_{9/2}$ spin alignments with no backbending or upbending. In contrast, for $T=1$ pairing $g_{9/2}$ alignments produce a large backbend. Because the experimental spectrum does not have a backbend or upbend, it does not follow that there are no spin alignments.

It has been shown that a small neutron excess weakens the $T=0$ pair mode relative to the $T=1$ pair mode [33]. Therefore it is possible that for neighboring isotopes such as ^{82}Zr or ^{84}Zr the $T=0$ pairing might be sufficiently weakened that the $T=1$ pair band remains lower in energy than the $T=0$ pair band until a spin which is much higher than $5\hbar$. It is also possible that the $T=0$ pair band does not exist for these isotopes. In these scenarios, the yrast band of these isotopes would follow the $T=1$ pair band, and the yrast band would then probably have a backbend between spins 8 and 14.

G. Deformation

The quadrupole deformation parameters β and γ are shown in Figs. 18 and 19. The convention is that $\gamma=60^\circ$ is oblate collective and $\gamma=-60^\circ$ is oblate noncollective. At spin $I=0$ all of the bands have a prolate axially symmetric shape. Rotation introduces a small amount of triaxiality. At low spins the $T=0$ pair band and $T=1$ pair band have very similar deformations. Even at high spins the two bands have deformations which are not dramatically different.

IV. CONCLUSIONS

HFB calculations for ^{80}Zr find a ground state band with $T=1$ pairing and an excited band with $T=0$ pairing. The bands cross at spin $I \approx 5\hbar$, providing a ‘‘phase transition’’ from $T=1$ pairs for $I < 5\hbar$ to $T=0$ pairs for $I > 5\hbar$. There is also a $T=0+T=1$ pair band, which forms an envelope to

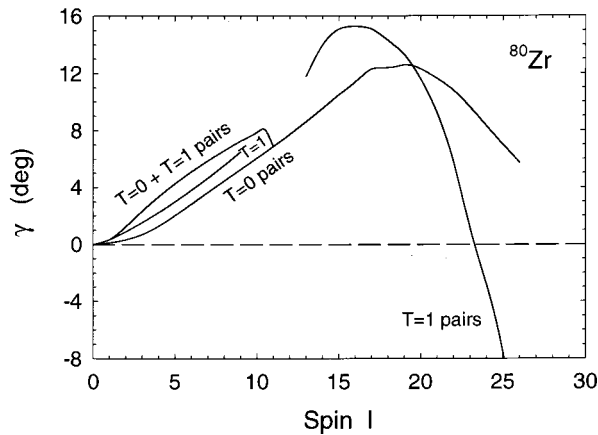


FIG. 19. Quadrupole deformation parameter γ for the $T=0$ pair band, the $T=1$ pair band, and the $T=0+T=1$ pair band.

the $T=1$ pair band and the $T=0$ pair band. In this band there is a more gradual transition from $T=1$ pairs at $I=0$ to $T=0$ pairs at high spins, with $T=0$ pairs and $T=1$ pairs coexisting at intermediate spins.

The Coriolis antipairing effect breaks the $T=1$ pairs, but there is no CAP effect for $T=0$ pairs in which the n and p occupy identical space-spin orbitals. The $T=1$ pair band backbends and has $g_{9/2}$ spin alignments. Even though the $T=0$ pair band does not backbend or upbend, it still has $g_{9/2}$ spin alignments. This demonstrates that if a rotational band does not have a backbend or upbend, it does not necessarily follow that there are no spin alignments. The dominant pair angular momentum for the $T=0$ pair band is $J=5$, not $J=1$ or $J=J_{max}=9$, as was expected. In the $T=1$ pair band the lowest quasiparticle energy vanishes at $I \approx 6$. However, for the $T=0$ pair band the lowest quasiparticle energy is approximately constant with spin, and does not vanish. For rotating $N=Z=$ even nuclei, $T=0$ pairing produces a twofold degeneracy in the canonical orbital occupation probability v^2 , although $T=1$ pairing produces a fourfold degeneracy in v^2 . Rotation induces a significant breaking of time-reversal symmetry in the pair potential.

ACKNOWLEDGMENTS

This work was supported in part by the National Science Foundation.

-
- [1] A. L. Goodman, *Adv. Nucl. Phys.* **11**, 263 (1979), Secs. 4.11 and 5.2.
- [2] K. Nichols and R. Sorensen, *Nucl. Phys.* **A309**, 45 (1978).
- [3] K. Muhlhans, E. Muller, K. Neergard, and U. Mosel, *Phys. Lett.* **105B**, 329 (1981).
- [4] E. Muller, K. Muhlhans, K. Neergard, and U. Mosel, *Nucl. Phys.* **A383**, 233 (1982).
- [5] D. Rudolph *et al.*, *Phys. Rev. Lett.* **76**, 376 (1996).
- [6] D. Dean, S. Koonin, K. Langanke, and P. Radha, *Phys. Lett. B* **399**, 1 (1997).
- [7] K. Kaneko and J. Zhang, *Phys. Rev. C* **57**, 1732 (1998).
- [8] K. Kaneko, M. Hasegawa, and J. Zhang, *Phys. Rev. C* **59**, 740 (1999).
- [9] S. Frauendorf, J. Sheikh, and N. Rowley, *Phys. Rev. C* **50**, 196 (1994).
- [10] S. Frauendorf and J. Sheikh, *Phys. Rev. C* **59**, 1400 (1999).
- [11] S. Frauendorf and J. Sheikh, *Nucl. Phys.* **A645**, 509 (1999).
- [12] S. Frauendorf and J. Sheikh, *Phys. Scr.* **T88**, 162 (2000).
- [13] W. Satula and R. Wyss, *Phys. Lett. B* **393**, 1 (1997).
- [14] J. Terasaki, R. Wyss, and P. Heenen, *Phys. Lett. B* **437**, 1 (1998).
- [15] J. Sheikh and R. Wyss, *Phys. Rev. C* **62**, 051302(R) (2000).
- [16] A. L. Goodman, *Phys. Rev. C* **58**, R3051 (1998).
- [17] A. L. Goodman, *Phys. Rev. C* **60**, 014311 (1999).
- [18] A. L. Goodman, *Nucl. Phys.* **A230**, 466 (1974).
- [19] A. L. Goodman, *Nucl. Phys.* **A265**, 113 (1976).
- [20] A. L. Goodman, *Nucl. Phys.* **A186**, 475 (1972).
- [21] C. Bloch and A. Messiah, *Nucl. Phys.* **39**, 95 (1962).
- [22] E. Kirchuk, P. Federman, and S. Pittel, *Phys. Rev. C* **47**, 567 (1993).
- [23] C. Lister *et al.*, *Phys. Rev. Lett.* **59**, 1270 (1987).
- [24] R. Firestone *et al.*, *Table of Isotopes*, 8th ed. (Wiley, New York, 1996).
- [25] B. Mottelson and J. Valatin, *Phys. Rev. Lett.* **5**, 511 (1960).
- [26] A. Goswami, L. Lin, and G. Struble, *Phys. Lett.* **25B**, 451 (1967).
- [27] B. Banerjee, P. Ring, and H. Mang, *Nucl. Phys.* **A221**, 564 (1974).
- [28] S. Belyaev, *Mat. Fys. Medd. K. Dan. Vidensk. Selsk.* **31**, No. 11 (1959).
- [29] F. Stephens, *Rev. Mod. Phys.* **47**, 43 (1975).
- [30] C. Lister, S. Fischer, and D. Belamuth, in *Proceedings of the International Workshop on Selected Topics on $N=Z$ Nuclei*, Lund, 2000, edited by D. Rudolph (Lund University, Lund, 2000), p. 46.
- [31] D. Rudolph *et al.*, *Phys. Rev. C* **56**, 98 (1997).
- [32] G. de Angelis *et al.*, *Phys. Lett. B* **415**, 217 (1997).
- [33] H. Wolter, A. Faessler, and P. Sauer, *Phys. Lett.* **31B**, 516 (1970).